COMMUNICATION

Wafer-Level Patterned and Aligned Polymer Nanowire/ Micro- and Nanotube Arrays on any Substrate

By *Jenny Ruth Morber, Xudong Wang, Jin Liu, Robert L. Snyder*, and *Zhong Lin Wang**

Aligned nanowires (NWs) of inorganic semiconductor materials have profound applications in photonics, electronics, sensing, bioscience, and energy science.[1–7] A key requirement for these applications is the cost-effective growth of high-quality, patterned, and uniformly aligned NWs at large scale on a substrate that is technologically important. Growth of aligned inorganic NW arrays can be achieved using either the vapor-liquid-solid[8] and vapor-solid-solid[9] process at high temperature ($> \approx 500\,°C$) with the assistance of catalyst particles,[10] or the seed-assisted chemical growth at low temperature.[11] There is a growing need to fabricate high-performance polymer-nanowire (PNW) based nanodevices for flexible electronics and photonics, but the above approaches are likely inapplicable for such purposes. Although templating, chemical synthesis, and even a few ion-generating techniques have yielded some promising results,[12–15] there is a lack of simple and scalable techniques for producing high-quality and controllable PNW arrays with the ability to pattern these PNWs on a large scale. We report one-step, clean fabrication of wafer-level *patterned and aligned* PNW or polymer micro- and nanotube (PNT) arrays, which are created simply by exposing the polymer material to plasma etching. The formation mechanism of the PNWs/PNTs is suggested to result from a dependence of the cone-shaped interaction volume between the ion and the polymer on its local incident-angle at the modulated surface. Our technique is capable of fabricating PNW arrays of any polymer on any material substrate. The aligning and patterning procedure provides a powerful and industrial nanofabrication technique that could lead to high-performance polymer-based flexible electronics, optoelectronics, sensors and photonics that can be fully integrated with silicon technology.

Fabrication of PNW arrays of functional polymers has important applications ranging from printable electronics, to implantable synthetic human muscles, to sensors and wires in smart clothing.[16–21] Thin films of conductive polymers such as PEDOT:PSS (poly(3,4-ethylenedioxythiophene) poly(styrenesulfonate)) have been used to develop organic light-emitting diodes (OLEDs), flexible displays, and organic solar cells.[22] Semicrystalline PVDF (polyvinylidene difluoride) is widely exploited for its high Young's modulus and unique piezoelectric properties.[23] While currently all organic devices are based on thin film configuration, patterned and aligned PNWs are expected to be perfect candidates for improving and integratable miniaturization of flexible electronics, including sensing textiles, biofeedback devices, and flexible displays.[24]

Our approach for producing wafer-level *aligned* PNWs is through a one-step inductively coupled plasma (ICP) reactive ion etching process. The polymer nanowire array was fabricated in an ICP reactive ion milling chamber with a pressure of 10 mTorr (1 Torr = 133.3 Pa). Ar, O_2, and CF_4 gases were released into the chamber as etchants at flow rates of 15 sccm (standard cubic centimeters per minute), 10 sccm, and 40 sccm, respectively.[25,26] A middle ground between purely chemical wet etching and purely physical ion-beam milling, plasma etching incorporates both a chemical etch component in the form of highly reactive neutral radicals, and a physical component in the form of plasma-generated ions.[25] Our system input gases included CF_4, O_2, and Ar. CF_4 is commonly used as a chemical etchant for ICP silicon processing as fluorine radicals created in the plasma react easily with Si. Oxygen is added in smaller quantities to remove unwanted polymer deposition created during treatment. For polymer ICP processing, atomic oxygen radicals generated from the oxygen gas are generally accepted to be the primary etchants. CF_4 is also frequently added to the mixture, as it has been shown to improve etch rates by increasing oxygen atom concentration. Excess fluorine, however, can slow the process by competing with oxygen for available polymer attack sites.[26] In both systems, inert gasses such as Ar-form positive ions are incorporated to serve as a physical component to assist in the material degradation process. One power source (400 W) was used to generate dense plasma from the input gases. A second power source (100 W) applied a voltage of approximately 600 V to accelerate the plasma toward the substrate. Both power sources operated at a frequency of 13.5 MHz. Helium gas also simultaneously flowed at the back of the substrate to maintain a temperature of 60 °C during fabrication.

Figure 1a shows a scanning electron microscopy (SEM) image of a PNW array of PEDOT:PSS with diameters of ≈ 400 nm and lengths $\approx 2\,\mu m$. All of the PNWs are perpendicular to the substrate, which is a 4 inch silicon wafer as shown in the bottom inset in Figure 1a. The PNWs have a fairly uniform size and distribution on the substrate. Longer PNWs should be possible at longer exposures as long as the starting polymer film is of appropriate thickness. Several processing times (1, 5, 15, and 25 min) were successfully used to generate the PNWs, with longer treatment generally corresponding to longer structures (Fig. S1).

The fabrication process is not limited by the chemical structure of the polymers. With no variation in processing parameters, we have successfully utilized this method to fabricate PNWs of several typical polymer compositions with diverse functionalities. Figure 1a–g show SEM images of the PNW made from polymers

[*] Prof. Z. L. Wang, Dr. J. R. Morber, Dr. X.-D. Wang, Dr. J. Liu, Prof. R. L. Snyder
School of Materials Science and Engineering
Georgia Institute of Technology
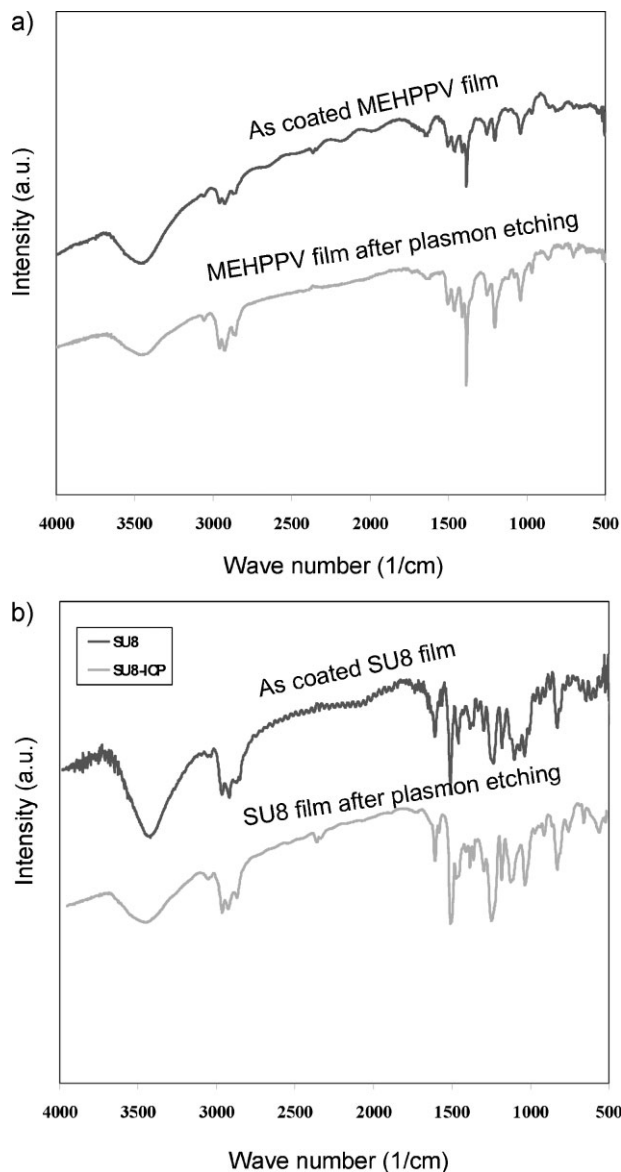Atlanta GA 30332-0245 (USA)
E-mail: zlwang@gatech.edu
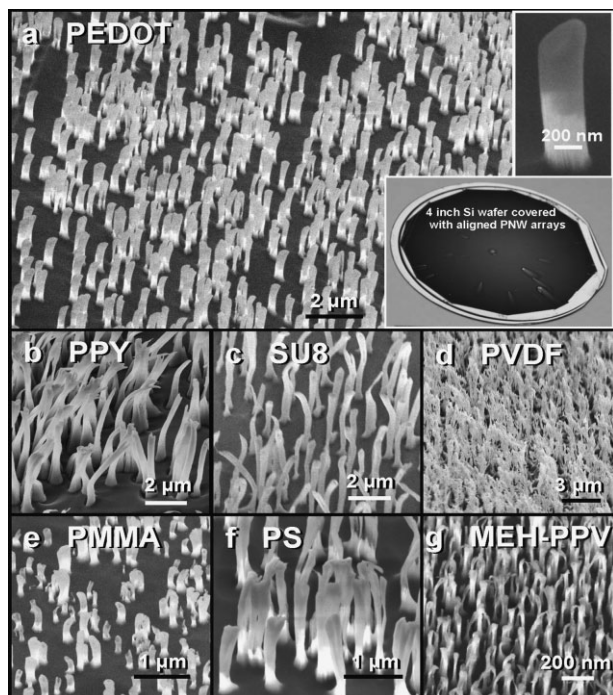
Figure 1. A series of SEM images demonstrating successful nanowire array formation for a variety of conductive and non-conductive polymers using the presented technique. a) PEDOT:PSS (poly(3,4-ethylenedioxythiophene) poly(styrenesulfonate)), b) PPY (polypyrrole), c) SU8 (1-methoxy-2-propyl acetate), d) PVDF (polyvinylidene difluoride), e) PMMA (Poly(methylmethacrylate)), f) PS (polystyrene), and g) MEH-PPV (poly(2-methoxy-5-(2′-ethylhexyloxy)-1,4-phenylenevinylene)). The top inset in a) is a single PEDOT:PSS NW showing a uniform diameter along its length. The bottom inset in a) is an optical image of a 4 inch wafer that is fully covered with aligned PNWs (darker area), fabricated by a one-step process.

Figure 2. a,b) FTIR spectra of MEHPPV film and SU8 film, respectively, before and after plasma etching, showing no detectable change in chemical nature of the polymers.

of PEDOT:PSS, PPY, SU8, PVDF, PMMA, PS, and MEH-PPV, respectively. Though not an exhaustive sample, these polymers differ greatly with regard to their chemistry and conductivity, underscoring the method's adaptabilty. PS is a rigid economic plastic for physical models as well as photonic crystals. SU8 and PMMA are commonly used as resists for photo- and electron beam lithography, respectively. PVDF is a dielectric piezoelectric and pyroelectric material for flexible sensors and actuators. PPY is a conductive, ionic electroactive polymer with potential application in humidity sensing, synthetic muscles, and cell manipulation. The remaining polymers are widely used components in organic electronics, such as PEDOT:PSS, a transparent, conductive polymer with high ductility, and MEH-PPV an optoelectronic polymer for OLEDs and organic solar cells.

FTIR spectra show no change in chemical nature of the polymer after plasma etching. Figure 2a and b show the FTIR spectra of MEHPPV film and SU8 film, respectively, before and after plasma etching, showing no detectable change in chemical nature of the polymer.
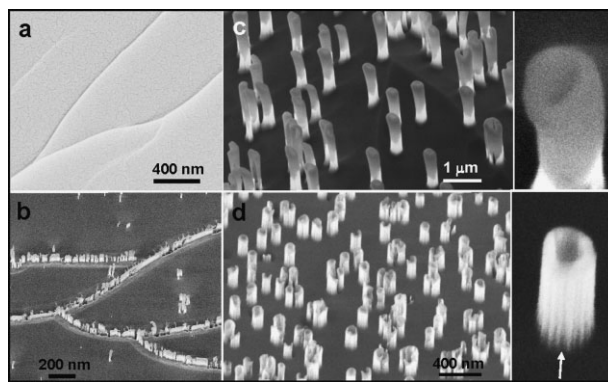
Our approach produces *patterned* PNW arrays at wafer-level, which is essential for integration with silicon and other materials based micro- and nano-technology. We first designed patterns on polymer surfaces by scratching using a micro-tip. A micro-manipulator equipped with a 1-μm tungsten needle tip was used

to draw a rectangular-like pattern on a 50-μm thick PS film, which was spin-coated on a silicon substrate. After 20-minute Plasma-Therm inductively coupled plasma (ICP) etching, PS PNWs were formed along the lines scratched by the manipulator tip, as shown in Figure 3a. The PNWs were typically single lines along the scratched path, while the unscratched area remained flat, as shown in Figure 3b. All of the PNWs in the patterned lines exhibited a fairly uniform diameter of ≈ 200 nm and height of ≈ 5 μm. Besides the direct-writing patterning technique, other bottom-up processes were also discovered to generate aligned PNW patterns. For example, ring patterns were created by applying air bubbles on polymer surfaces. Drying of air bubbles left circular protrusions, which formed aligned PNW rings (Fig. 3d). The smallest ring pattern had a diameter of ≈ 1 μm, while the width of the PNWs was less than 100 nm (Fig. 3e). Most PNWs
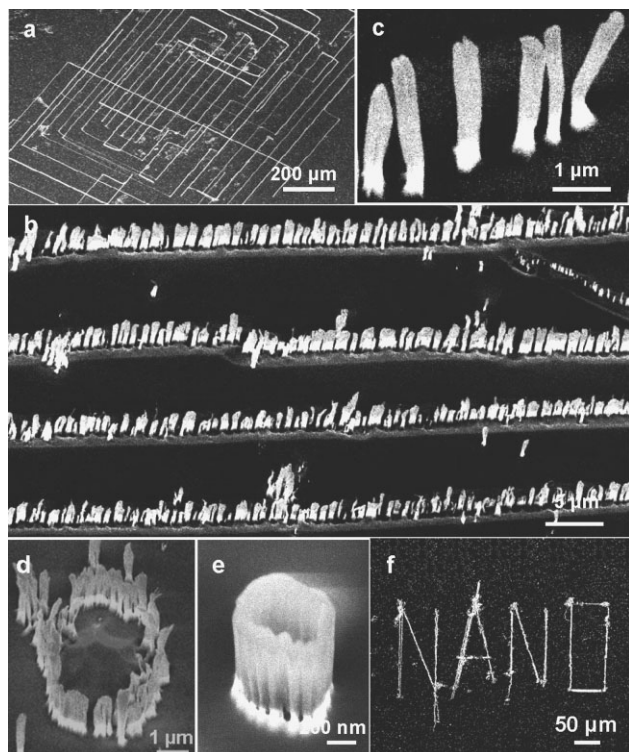
Figure 3. Patterned fabrication of PS nanowire arrays in artificial false color. a) Scratching the flat polymer surface with a microneedle in a complex design yields corresponding nanowire formation along the scratched lines. The unscratched area does not form wires. b) A higher magnification image of single nanowire rows formed along patterned scratches. c) A high magnification SEM image of patterned nanowires showing size and morphology. d) A patterned circle of polymer nanowires. e) Aligned PNW rings formed from bubbles induced on polymer surface. f) A large "NANO" pattern formed by scratching the polymer surface by hand.

Figure 4. Experimental observations of fine morphologies of the formed PNWs and PNTs that are important for the proposed formation mechanism. a) Surface of a PS film showing wrinkles/ridges prior to ion bombardment. b) Surface of a PS film showing the formation of PNWs along the wrinkles/ridges on the surface after ion bombardment. c) Presence of dips at the top ends of PEDOT NWs. d) Formation of MEH-PPV PNT arrays as a result of plasma etching, where the parallel tracks created by the incident ions are clearly visible.

were "fused" together forming a continuous circular wall. Large PNW patterns were also generated through handwriting, such as the letters "NANO", which was simply created by hand-sculpting a PS thin film surface using a fine needle (Fig. 3f). Our data show that the PNW formation is due primarily to anisotropic ion bombardment of the polymer surface owing to local variation in curvature, which may possibly be accelerated by additional chemical etching.

The patterned PNWs can also be generated by conventional masking technology, which defines areas covered or not covered by PNWs by simply blocking species from reacting with the polymer film (Fig. S2). Owing to the vertical trajectory of ions, mostly sharp edges were observed. Half-pillar-shaped features were engraved along the side wall indicating the vertical trajectory of ion bombardments (Fig. S2). The mask pattern can also be easily reversed, analogous to the use of negative photoresist in lithography. By stamping/touching a copper transmission electron microscopy (TEM) grid on a uniform PS film and then peeling it off, the contact area became rough, which produced high-density PNW arrays after etching (the white area in Fig. S3a and S3b; see the enlarged SEM image in Fig. S3c). Only a few PNWs were formed on the flat untouched surfaces (the black area in Fig. S3a). Such a stamping approach can be applied to generate

PNW patterns as small as a few micrometers with clear distinguishing boundaries (Figs. S3c and S2).
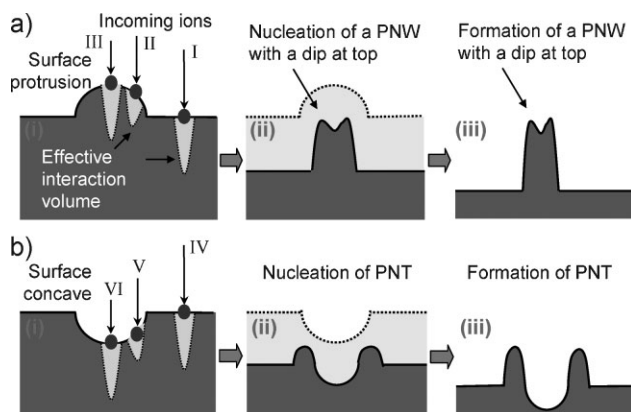
A series of experiments have been carried out to reveal the possible formation mechanism of the PNW arrays. The plasma etching has been observed to particularly amplify the areas that are either bumpy or with interfaces or imperfections, which become more pronounced after ion beam bombardment. Experimentally, PNWs tend to grow at areas that have ripples or other surface roughness in the starting material (Fig. 4a). Although the protrusion of such wrinkles is only tens of nanometers, it creates a large enough change in local geometry that it leads to the formation of PNWs (Fig. 4b). Because sputter yields are highly dependent on the incident beam angle, any initial roughness of the sample such that the material is positioned at an angle off-perpendicular to the beam will experience a difference in the effective ion beam incidence and become more pronounced after milling. Chemically reacting species, however, are known for their isotropic etching profiles, which would tend to hinder nanowire formation.

Furthermore, detailed examination reveals that PNWs of PEDOT have dips at their top ends (Fig. 4c). Polymer NT arrays of MEH-PPV have been fabricated (Fig. 4d), which show a hollow tubular structure, with the wall of the tube made of tracks parallel to its axis, indicating that the interaction of the incident ions with the polymer is confined in a "cigar"-shaped volume along its path.

Theoretically, the formation process of a regular ripple pattern on a solid surface as a result of ion bombardment has been described by the Bradley–Harper (BH) model,[25] in which the pattern results from a balance between roughening due to the removal of surface material and smoothing by surface diffusion. A surface instability is induced by the curvature dependence of the sputter yield, because the local etching rate is higher at a local dip than at a protrusion. This leads to an amplification of initial surface modulations and to a roughening of the surface. In reference to the experimental facts presented in Figures 1–4, we propose the following model about the formation of the PNWs and PNTs.

It is known that the interaction of charged ions with polymer can involve processes such as physical sputtering-off, local ionization, kinetic energy transfer, and stimulated chemical reaction. To comprehensively represent the resultant effect of these processes, we assume that the interaction between an incoming ion and the polymer is confined within a "cone-shaped" volume along its path, as evidenced by the surface structure observed at the surface of the PNT inset in Figure 4d (indicated by an arrowhead). The length of the cone-shaped interaction volume (CSIV) depends on the local incident angle of the ion at the surface, because the backscattering of the ion at the surface can reduce its probability to penetrate into the polymer. The highest penetration is when the ion is normal to the surface. We now consider the case that the polymer surface has a protrusion (Fig. 5a(i)), around which three possible incident ion locations are marked: track I is a normal incidence on a flat surface, track II is on the side surface of the protrusion, and track III is at the top of the protrusion. Ions I and III are along the normal of the local surfaces, thus their CSIV is long along the ion path, while ion II has a shorter CSIV because its local incident angle is off the surface normal. If the polymer covered by the CSIV is being removed across the surface, a PNW is formed and its top has a dip due to the long CSIV of ion III (Fig. 5a(ii)). The side wall of the PNW is likely to have fluoride adsorption, which may protect the side from transverse etching (see Fig. S2).[26] A continuation of etching in the depth direction results in the formation of a PNW (Fig. 5a(iii)) that has a dip at its top, as observed experimentally in Figure 4c.

We now consider an alternative case that the polymer surface has a concave or dip at the initial thin film surface (Fig. 5b(i)). Ions IV and VI are normal to the local surface, but ion V is off the normal. Analogous to the ions I, II, and III, the local CSIV for ions IV and VI is longer than that of ion V. The profile created by this etching results in a nucleation of a ring on the surface (Fig. 5b(ii)).

A continuous etching along the ion path results in a longer NT (Fig. 5b(iii)), as observed experimentally in Figure 4d.
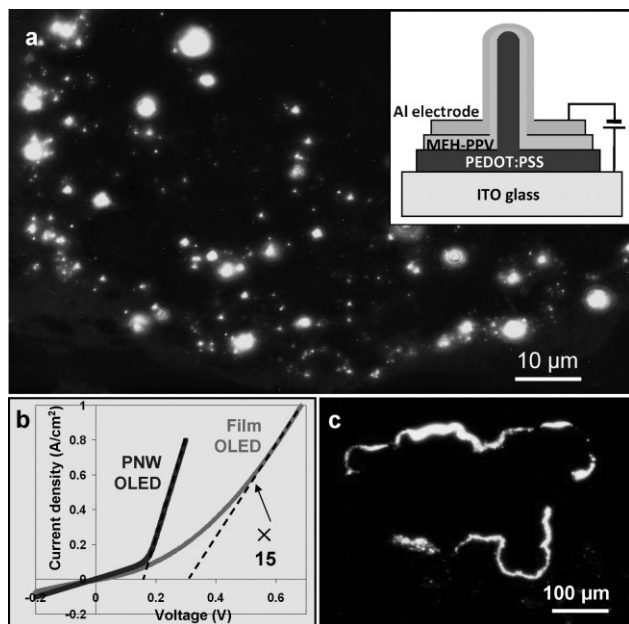
For a polymer film with wrinkle-type ridges, a non-uniform bombardment of the ions at beginning could produce local dips along the ridge. Amplification of such dips by ion etching following the process shown in Figure 4f may result in lines of PNWs, instead of a continuous wall (see Fig. 4b).

In addition to the dominant physical process, chemical effect is also important. During etching, oxygen has to present to decompose the polymer and accelerate physical milling (Fig. S4). No PNW was observed when a polymer sample was treated with Ar only (Fig. S4a). Polymer exposure to only O_2 created arrays of PNWs (Fig. S4b), though with a lower density than those created with all gasses (Fig. S4d). Samples treated with both O_2 and Ar also exhibited PNW formation (Fig. S4c), but these were sparse, thin, and of low quality, indicating a very high relative milling rate for these samples. The inability of argon to create nanowires alone, coupled with previous evidence that physical milling plays an active role in nanowire formation when all gasses (Ar, O_2, and CF_4) are present, implied that physical collisions (knock off), charge interaction and even chemical processes are at work. All of these processes are characterized by the cone-shaped effective interaction volume around the ion trajectory, as shown in Figure 5.

The successful growth of aligned PNWs from conductive or semiconducting polymers opens a great opportunity for developing polymer-based flexible nano-electronic devices. Traditionally, most flexible electronics such as OLEDs, organic solar cells, organic transistors, etc. are built on polymer thin films. Replacing the thin films with PNW arrays can significantly increase the contact surface area, enhancing charge transport properties. Solar cells based on nanowires have been shown to exhibit more efficient charge carrier separation and increased forward bias compared to thin film controls.[27] Using PNW arrays made from PEDOT:PSS, we have fabricated an organic PNW-OLED device (inset in Fig. 6a). For the fabrication of OLED, a layer of PEDOT:PSS was spin coated onto ITO coated glass and baked for 10 minutes at 120 °C. 20-minute ICP etching created vertically aligned PEDOT:PSS NWs with typical lengths of ≈5 μm and diameters of ≈400 nm. MEH-PPV was then spin coated on the PNW arrays followed by another 10-minute baking at 120 °C. Finally, an aluminum electrode was deposited on top of the polymer layers via thermal evaporation in vacuum. For comparison, a thin film OLED built from the same materials was also tested under the same conditions.

For comparison, a thin film OLED built from the same materials was also tested under the same conditions. The PNW-OLED demonstrated an ability to transport a maximum current density ≈40 times greater than what the thin film OLED could handle (Fig. 6b).

By applying a DC voltage between the alumina electrode and ITO glass, the PNW-OLED generated many bright but tiny yellow dots of light (Fig. 6a). This is because the PEDOT:PSS NWs provided a large surface area contacting the MEH-PPV layer where numerous photons were generated. The emission was possibly from the PNW tips owing to the enhanced local electric field (Fig. S5a). Thus, each PNW produced one bright spot covering an area of less than 1 μm × 1 μm, as the small yellow dots on Figure 6a suggest. In the case that PNWs were bundled

Figure 5. Proposed mechanism about the formation of PNWs and PNTs by plasma etching. Schematic cross-sectional diagrams describing the formation of a) PNW and b) PNT arrays at a polymer surface that has a protrusion and dip local surface modulation, respectively. The core of this mechanism is using of a cone-shaped interaction volume to represent the physical and chemical processes excited by the charged ion. More importantly, considering the dependence of ion penetration probability into the polymer as a function of its incidence angle at the surface, the length of the interaction volume is reduced once the ion track is off the surface normal direction. This is the fundamental of the proposed mechanism.

Figure 6. The PNW arrays were used to create a working OLED device. a) Small and large dots of bright yellow light are likely to be emitted from single nanowires and nanowire bundles, respectively. A schematic of the device is shown in the inset. b) The PNW device was found to demonstrate a significantly lower turn-on voltage and higher current-density capacity compared to a thin film control fabricated under the same conditions. The film OLED curve is magnified 15 times to emphasize the difference in turn-on voltage compared to the PNW device. c) Patterned light output from the OLED showing the outline of a "US map." The OLED data recorded at 3.5 V were clearly visible to the naked eye.

close to each other (Fig. S5b), the small individual dots could not be distinguished. Instead, bigger and brighter light spots were recorded (Fig. 6a). Utilizing the advantage of easy patterning, micrometer-sized light images can be created with this technique. Figure 6c shows an optical microscope image of an illuminated "US map" composed by thick lines of PNWs that were built into a PNW-OLED. The success of fabricating PNW-OLED indicates that the radiation damage introduced by plasma for fabricating the PNWs, if any, is negligible at least for the current example.

In summary, there are outstanding technological needs to seek simple, scalable techniques for fabrication and patterning of aligned polymer nanowires, especially conductive polymers, as integral tools for applications such as flexible electronics and LEDs, immunosensors, synthetic muscles, and electronic cell manipulation. We report a simple technique for fabrication of PNW arrays on a substrate of any material that can accommodate films of polymer material. Patterned PNW arrays of almost any polymer can be fabricated on any substrate by either micro-tip surface engineering or stamping induced surface roughness. The formation mechanism of the PNWs/PNTs is suggested to be due to a dependence of the cone-shaped interaction volume between the ion and the polymer on its local incident-angle at the modulated surface. Our approach is a one-step method for cost-effective and large-scale fabrication of patterned and aligned

PNW/PNT arrays on general substrates that can be easily integrated with silicon technology, having potential applications in OLEDs, flexible electronics, biosensors and synthetic muscles.

[1] Y. Cui, Q. Q. Wei, H. K. Park, C. M. Lieber, *Science* **2001**, *293*, 1289.
[2] F. Patolsky, B. P. Timko, G. Yu, Y. Fang, A. B. Greytak, G. Zheng, C. M. Lieber, *Science* **2006**, *313*, 1100.
[3] P. J. Pauzauskie, P. Yang, *Mater. Today* **2006**, *9*, 36.
[4] J. Goldberger, A. Hochbaum, R. Fan, P. Yang, *Nano Lett.* **2006**, *6*, 973.
[5] Y. Qin, X. D. Wang, Z. L. Wang, *Nature* **2008**, *451*, 809.
[6] X. D. Wang, J. H. Song, J. Liu, Z. L. Wang, *Science* **2007**, *316*, 102.
[7] A. I. Persson, M. W. Larsson, S. Stenström, B. J. Ohlsson, L. Samuelson, L. R. Wallenberg, *Nat. Mater.* **2004**, *3*, 677.
[8] R. S. Wagner, W. C. Ellis, *Appl. Phys. Lett.* **1964**, *4*, 89.
[9] S. Kodambaka, J. Tersoff, M. C. Reuter, F. M. Ross, *Science* **2007**, *316*, 729.
[10] X. D. Wang, C. J. Summers, Z. L. Wang, *Nano Lett.* **2004**, *4*, 423.
[11] Z. R. R. Tian, J. A. Voigt, J. Liu, B. Mckenzie, M. J. Mcdermott, M. A. Rodriguez, H. Konishi, H. Xu, *Nat. Mater.* **2003**, *2*, 821.
[12] J. Liu, Y. Lin, L. Liang, J. A. Voigt, D. L. Huber, Z. R. Tian, E. Coker, B. Mckenzie, M. J. Mcdermott, *Chem. Eur. J.* **2003**, *9*, 604.
[13] J. C. Hulteen, C. R. Martin, *J. Mater. Chem.* **1997**, *7*, 1075.
[14] A. K. Wanekaya, W. Chen, N. V. Myung, A. Mulchandani, *Electroanalysis* **2006**, *18*, 533.
[15] D. J. Lipomi, R. C. Chiechi, M. D. Dickey, G. M. Whitesides, *Nano Lett.* **2008**, *8*, 2100.
[16] Y. Berdichevsky, Y. H. Lo, *Adv. Mater.* **2006**, *18*, 122.
[17] E. Smela, *Adv. Mater.* **2003**, *15*, 481.
[18] D. G. Anderson, J. A. Burdick, R. Langer, *Science* **2004**, *305*, 1923.
[19] E. W. H. Jager, E. Smela, O. Inganas, *Science* **2000**, *290*, 1540.
[20] J. H. Ahn, H. S. Kim, K. J. Lee, S. Jeon, S. J. Kang, Y. Sun, R. G. Nuzzo, J. A. Rogers, *Science* **2006**, *314*, 1754.
[21] K. Ramanathan, M. A. Bangar, M. Yun, W. Chen, N. V. Myung, A. Mulchandani, *J. Am. Chem. Soc.* **2005**, *127*, 496.
[22] M. Gross, D. C. Müller, H. G. Nothofer, U. Scherf, D. Neher, C. Bräuchle, K. Meerholz, *Nature* **2000**, *405*, 661.
[23] K. Tashiro, M. Kobayashi, H. Tadokoro, E. Fukada, *Macromolecules* **1980**, *13*, 691.
[24] A. L. Briseno, S. C. B. Mannsfeld, M. M. Ling, S. Liu, R. J. Tseng, C. Reese, M. E. Roberts, Y. Yang, F. Wudl, Z. Bao, *Nature* **2006**, *444*, 913.
[25] R. M. Bradley, J. M. E. Harper, *J. Vac. Sci. Technol. A* **1988**, *6*, 2390.
[26] R. D'Agostino, *Plasma Deposition, Treatment, and Etching of Polymers*, Academic, Boston **1990**.
[27] C. J. Novotny, E. T. Yu, P. K. L. Yu, *Nano Lett.* **2008**, *8*, 775.

WILEY InterScience®
DISCOVER SOMETHING GREAT